analytical chemistry

Article

pubs.acs.org/ac

Electrochemical and Density Functional Theory Investigation on High Selectivity and Sensitivity of Exfoliated Nano-Zirconium Phosphate toward Lead(II)

Lei Wang,[†,∥] Wei-Hong Xu,[†,∥] Ran Yang,[†] Ting Zhou,[‡] Dong Hou,[‡] Xiao Zheng,*[,‡,§] Jin-Huai Liu,[†] and Xing-Jiu Huang*[,†]

[†]Research Centre for Biomimetic Functional Materials and Sensing Devices, Institute of Intelligent Machines, Chinese Academy of Sciences, Hefei, Anhui 230031, P.R. China

[‡]Hefei National Laboratory for Physical Sciences at the Microscale, Department of Chemical Physics, University of Science and Technology of China, Hefei, Anhui 230026, P.R.China

[§]Guizhou Provincial Key laboratory of Computational Nano-Material Science, Institute of Applied Physics, Guizhou Normal College, Guiyang, 550018, P.R.China.

Supporting Information

ABSTRACT: A new strategy on the understanding of selective and sensitive identification of Pb(II) using combined experimental and theoretical efforts is described. Amorphous phase formation of exfoliated nano-zirconium phosphate (ZrP) has been prepared via a hydrothermal process and subsequent intercalation reaction. Exfoliated ZrP was used as coating on the electrode surface, and it was found to be selective and sensitive for Pb(II) detection due to its selective adsorption ability. To better and scientifically understand the microscopic adsorption mechanism, density functional theory (DFT) calculations about the details of chemical interactions between heavy metal ions and exfoliated ZrP were carried out at an atomistic level. It is verified that the exfoliated ZrP shows the strongest adsorption capability toward Pb(II) among all heavy metal ions, thereby resulting in selective detection consequently. With our combined experimental and theoretical efforts, we are able to provide a new route to realize the improved selectivity in electrochemical sensing of toxic metal ions.

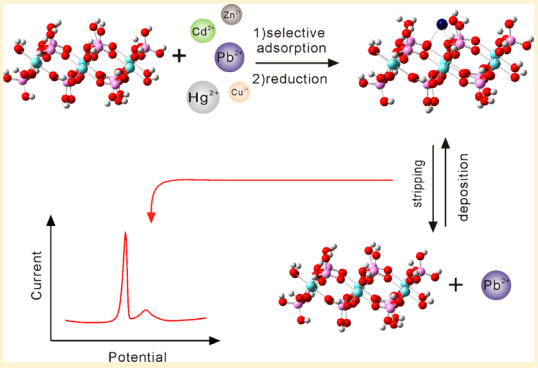

Direct, selective, and sensitive determination of lead is imperative due to its high toxicity for biological systems, especially for children.[1−4] Electrochemical technique has been recognized as a promising method for ultratrace and on-site analysis of lead due to portability, high sensitivity, good selectivity, low cost, and suitability. In order to realize a more sensitive and selective electroanalysis, there is a trend to explore composite-modified electrodes with some special but unproven properties. Novel modifiers, such as organic, inorganic compounds, and biomolecules, with characteristic functional groups constantly provoke increasing research interest,[1,5−9] although a number of studies have demonstrated that appropriate materials are highly beneficial for electrochemical detection because of their selective adsorption properties.[10−12] Unfortunately, the detailed mechanisms on how selective adsorption results in selective response remain largely hazy at the present stage. In addition, it should also be noted that some of the successful coatings on modified electrodes show dramatically increased currents and increased sensitivity simply ascribed to the increased microscopic surface area or high surface free energy. In short, these findings tilt not to empiricism but scientism. Hence, to better and scientifically understand the unproven properties of the modified electrodes, developing techniques with scientific essence in analytical chemistry is in great demand. Achieving such a break through requires the design and implementation of new experimental techniques in conjunction with theoretical investigations. Here, we outline a combined anodic stripping voltammetry (ASV) and theoretical investigation approach to analyze Pb(II) in water system. We fabricate an electrochemical platform based on a simple inorganic modifier, exfoliated zirconium phosphate (ZrP), for selective detection of lead ions (Pb(II)).

ZrP materials exhibit high adsorption capacity toward heavy metal ions and great selective adsorption toward Pb(II). These include two-layer compounds (α-ZrP, γ-ZrP) and their derivatives whose catalytic properties, intercalation chemistry, ion exchange capacities, and some other properties have been widely investigated.[13−21] It has been recognized that layer compounds after exfoliation can efficiently reveal active functional groups and improve reactivity. However, little has

Received: December 20, 2012
Accepted: March 20, 2013
Published: March 20, 2013

   dx.doi.org/10.1021/ac3037014 | *Anal. Chem.* 2013, 85, 3984−3990

been done on the electrochemical applications, which may be because the poor conductive properties of zirconium phosphate materials restrict their applications as electrochemical sensors.

In this work, we report the stripping signals for selective identification of Pb(II) using exfoliated ZrP. First principles theoretical studies at an atomic level are expected to provide insightful information on the interaction between the Pb(II) and ZrP surface for scientific understanding of the underlying microscopic mechanisms. The atomistic details of chemical interactions between metal ions and the ZrP surface are investigated by density functional theory (DFT) calculations. Our combined electrochemical and theoretical studies affirm that the selective adsorption of Pb(II) ions on exfoliated ZrP indeed leads to sensitive and selective detection.

EXPERIMENTAL SECTION

Chemicals. All chemicals used were of analytical grade and were used as received without any further purification. All chemicals were purchased from Sinopharm Chemical Reagent Co., Ltd. (China). These were zirconyl chloride octahydrate ($ZrOCl_2{\cdot}8H_2O$, 98%), phosphoric acid (85%), $Pb(NO_3)_2$, $3CdSO_4{\cdot}8H_2O$, $Cu(NO_3)_2$, $Hg(NO_3)_2$, $Zn(NO_3)_2$, and 25 wt % tetramethylammonium hydroxide (TMA^+OH^-) solution. Acetate buffer solutions of 0.1 M for different pH were prepared by mixing stock solutions of 0.1 M HAc and NaAc. All solutions were prepared with deionized water of resistivity not less than 18.2 MΩ cm.

Apparatus. Electrochemical experiments were recorded using a CHI 660D computer-controlled potentiostat (ChenHua Instruments Co., Shanghai, China) with a standard three electrode system. A bare glassy carbon electrode (GCE, diameter of 3 mm) or modified GCE served as a working electrode; a platinum wire was used as a counter-electrode with a saturated Ag/AgCl electrode (ChenHua Instruments Co., Shanghai, China) completing the cell assembly.

X-ray diffraction (XRD) patterns were recorded in the range of $2\theta = 5-30°$ with a Philips X'Pert X-ray diffractometer, using Cu Kα ($\lambda_{K\alpha 1}$ = 1.5418 Å) as the radiation source. Transmission electron microscopy (TEM) and energy-dispersive spectrometer (EDS) were recorded using a JEM-2010 transmission electron microscope operated at 200 KV (Quantitative method: Cliff Lorimer thin ratio section). Atomic force microscopy (AFM) images were carried out using Nanoscope III (Digital Instruments, Veeco Metrology). X-ray photoelectron spectroscopy (XPS) analyses of the samples were conducted on a VG ESCALAB MKII spectrometer using an Mg Kα X-ray source (1253.6 eV, 120 W) at a constant analyzer. pH value was measured using pH meter (Model: PHS-3C).

Synthesis of Layered α-ZrP and Exfoliated ZrP. Layered α-ZrP was first prepared according to the literature.[22] Briefly, 3.0 g of $ZrOCl_2{\cdot}8H_2O$ was mixed with 30.0 mL H_3PO_4 (6.0 M) in a sealed Teflon lined pressure vessel and reacted at 200 °C for 24 h. Then the products were centrifuged, washed with water, and dried at 65 °C in an oven for further use. The pristine α-ZrP prepared was exfoliated by 25 wt % TMA^+OH^- solution in an aqueous dispersion under stirring at room temperature for about 7 h.[23] Then the products were washed and collected by centrifugation and dried at 65 °C prior to use.

Electrode Fabrication. The construction of exfoliated ZrP on the surface of GCE was performed as follows: 5 mg of exfoliated ZrP was suspended in 1 mL of distilled water to form a suspension. The suspension was then briefly sonicated for 30 s in order to disperse the nanocomposites. A 4 μL aliquot of this suspension was then pipetted onto the surface of a freshly polished GCE and evaporated at room temperature. Similar procedure was used to prepare layered α-ZrP-modified electrode.

Electrochemical Experiments. Square wave anodic stripping voltammetry (SWASV) was used for Pb(II) detection under optimized conditions. A deposition potential of −1.1 V was applied for 120 s to the working electrode by the reduction of Pb(II) in 0.1 M NaAc−HAc (pH 4.0). The anodic stripping (reoxidation of metal to metal ions) of electrodeposited metal was performed in the potential range of −1.0 to 0 V with step potential of 4 mV, amplitude of 25 mV, and frequency of 15 Hz. A desorption potential of 0 V for 150 s was performed to remove the residual metals under stirring condition. The individual detection of Zn(II), Cd(II), Cu(II), and Hg(II) has been performed at the same experimental conditions (except Zn(II) with a deposition potential of −1.3 V for 120 s. This is because only when deposition potential is more negative (100−300 mV) than the potential for stripping peak, metal ions could be deposited on the electrode surface in the deposition step. Generally, the stripping peak for Zn(II) emerges at around −1.1 V.). All experiments were performed at room temperature under air atmosphere.

Adsorption Measurements. All the adsorption experiments were carried out in glassy vials by using a batch technique. To start the experiment, 50 mg of the individual sorbent was introduced into 100 mL aqueous solutions containing heavy metal ions, and then the solutions were shaken at 298 K for 24 h to ensure the sorption process reach equilibrium. The solid and liquid phases were separated by centrifugation at 10000 rpm for 6 min, and the solid was dried at 65 °C for further XPS analysis. NaAc and HAc (0.1 M) were used to adjust the solution pH to 4.0 throughout the experiment.

Computational Details. All calculations were carried out using the Gaussian09 suite of electronic structure programs[24] and the SIESTA Program.[25]

All electronic structures were obtained at the unrestricted density functional theory level with the B3LYP exchange correlation functional.[26] Geometry optimizations were performed using Lanl2dz basis set. A relatively small basis set was found sufficient to obtain reasonable structures because the optimized structure was found rather insensitive to further increasing the size of basis set. The thermodynamical energetic data were obtained by B3LYP single point calculations with 6-31+G* basis set at the optimized structures. To take the solvent effect of water into account, we applied the polarizable continuum model (PCM) of Tomasi and co-workers[27,28] to obtain the solvation free energy on the optimized geometry. The periodic structure relaxation of single layer ZrP was calculated by SIESTA using GGA-PBE exchange-correlation functional.[29]

RESULTS AND DISCUSSION

Figure 1 illustrates the selective electrochemical detection of Pb(II) by exfoliated ZrP. The adsorption of metal ions on ZrP surface is probed by square wave anodic stripping voltammetry (SWASV) technique. For instance, the adsorbed Pb(II) is reduced to Pb(0) at a certain potential, and the anodic stripping current associated with the reoxidation of Pb(0) identifies the amount of Pb(II) adsorbed on electrode surface. Among the most commonly involved heavy metal ions (e.g., Zn(II), Cd(II), Pb(II), Cu(II), and Hg(II)), Pb(II) was believed to

dx.doi.org/10.1021/ac3037014 | Anal. Chem. 2013, 85, 3984−3990

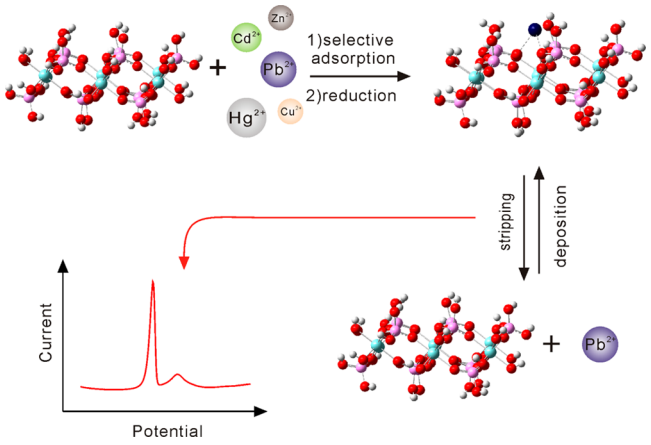

Figure 1. Schematic illustration of selective electrochemical detection of Pb(II) by exfoliated ZrP. The ball-and-stick models sketch the geometric structures of exfoliated ZrP with and without adsorbed metal ions.

have the highest priority to be adsorbed on the exfoliated ZrP surface due to its largest binding affinity.

Well-defined crystalline layered α-ZrP and amorphous exfoliated ZrP have been prepared via a hydrothermal process and subsequent intercalation reaction, respectively. Transmission electron microscope (TEM) images of layered α-ZrP depicted in Figure 2a show a regular fringe with a lateral dimension of 500−1000 nm, while for exfoliated ZrP sheets displayed in Figure 2b, the edges appear to be corroded in the similar lateral dimension. This may be ascribed to the impact of inevitable hydrolysis on the reactive edges.[30,31] Besides, the P/Zr ratio in layered α-ZrP is determined as approximately 2:1 by EDS analysis, which verifies its stoichiometry as $Zr(HPO_4)_2$, while the ratio in exfoliated ZrP is found to be less than 2 (Figure S1, Supporting Information). This is understandable because phosphate groups on the edges are accessible to base, so that hydrolysis occurs during exfoliation and releases a massive amount of P and negligible Zr into liquid phase, leaving the ratio of P/Zr below 2.[30] In addition, the thickness of the exfoliated ZrP is about 2.5 nm with the broken edges measured by atomic force microscopy, much thinner than layered α-ZrP, indicating that the pristine α-ZrP has been successfully exfoliated (Figure 2c). The disappearance of the typical diffraction peaks at 2θ = 11.7°, 19.8°, and 25° corresponding to the primary diffraction of the (002), (110), and (112) planes also demonstrates that the layered α-ZrP has been destroyed and exfoliation is completed (Figure 2d).[32−35] Meanwhile, the exfoliated ZrP is amorphous in contrast to the crystalline layered α-ZrP, as suggested by the corresponding electron diffraction patterns (insets in Figure 2a and b). To illustrate such a phase transition process, DFT calculations are carried out on periodic single layer ZrP. It is found that the positions of Zr atoms tend to be displaced significantly in the direction perpendicular to the layer due to the vanishing van der Waals interactions between layers after exfoliation. Therefore, it is very likely that the exfoliated single layer ZrP will undergo out of plane distortion to form wrinkles or stripes, leading to formation of amorphous phase. This is consistent with the XRD and TEM observations that the exfoliated ZrP only exhibits short-range ordering.

The surface modification of electrodes was characterized by cyclic voltammetry (CV) and electrochemical impedance spectra (EIS) in 5 mM $Fe(CN)_6^{3-/4-}$ containing 0.1 M KCl (Figure S2, Supporting Information). The decrease of anodic and cathodic peaks and the increase of the impedance compared with the bare glassy carbon electrode (GCE) indicate the poor conductivity of ZrP.

Initial detection experiments on modified electrodes are conducted by observing the SWASV signals in NaAc−HAc solution (Figure 3). A double stripping peak for Pb(II) detection is observed, one peak emerges at around −0.55 V and

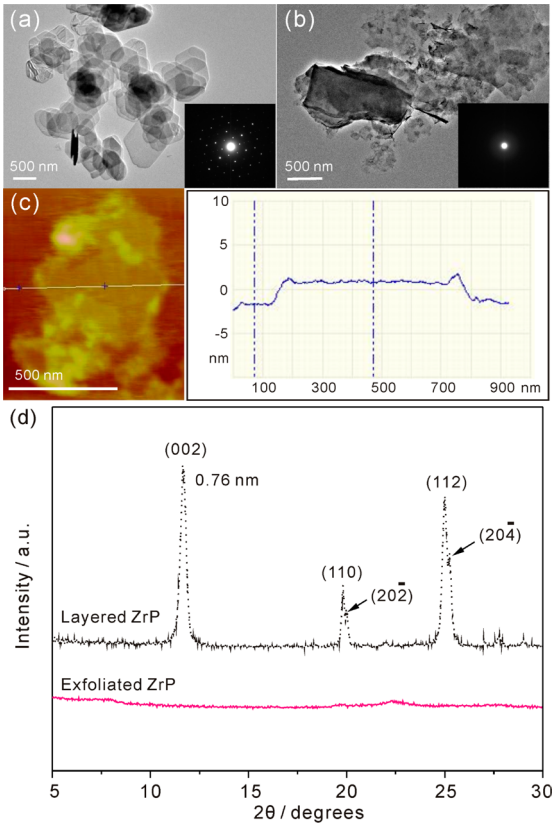

Figure 2. Representative TEM images of (a) layered α-ZrP and (b) exfoliated ZrP. The insets show the corresponding electron diffraction patterns. (c) AFM image of exfoliated ZrP with height profile. (d) XRD patterns of layered α-ZrP and exfoliated ZrP.

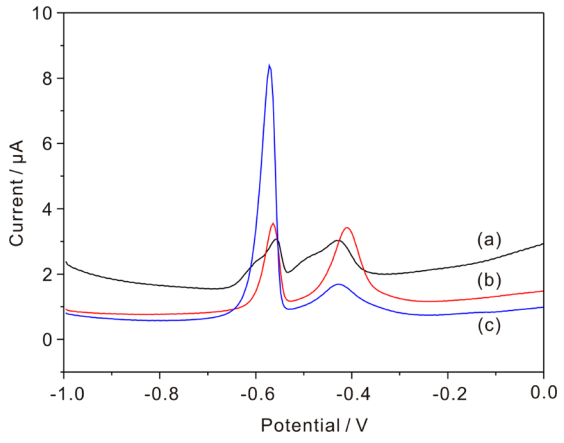

Figure 3. Typical SWASV responses of 0.8 μM Pb(II) at (a) bare (black line), (b) layered α-ZrP (red line), and (c) exfoliated ZrP-modified (blue line) GCE in 0.1 M NaAc−HAc solution (pH 5.0).

dx.doi.org/10.1021/ac3037014 | Anal. Chem. 2013, 85, 3984−3990

the other is around −0.42 V. This is intimately related to the different ZrP morphologies on the GCE surface, which reflect the complex nature of nucleation and growth of Pb nanoparticles on electrode surface.[36] In the following, we choose the characteristic peak at −0.55 V as the feature of Pb(II) to study the behavior of exfoliated ZrP. It is shown that peaks become more prominent as the GCE surface is modified by ZrP. This affirms that the Pb(II) adsorption ability of electrode surface is greatly enhanced with ZrP modification. Strikingly, the response performance of the exfoliated ZrP is found to be significantly improved over that of the layered α-ZrP. This is ascribed to the enhanced reactivity of the exfoliated ZrP and will be discussed later.

In the following sections, exfoliated ZrP-modified GCE is applied to optimize the conditions for the detection of Pb(II) (Figure S3, Supporting Information) and investigate the selectivity toward heavy metal ions. The voltammetric behavior of Pb(II) was investigated in three different supporting electrolytes at pH 5.0: 0.1 M NH_4Cl-HCl, phosphate, and acetate buffer solution. Optimal sensitivity is found in NaAc−HAc solution, where the stripping peak is well defined with strongest stripping signal (Figure S3a, Supporting Information). The specific pH-dependent behavior can be attributed to the specific adsorption mechanism of exfoliated ZrP, which is driven by the electrostatic attraction or complexation mechanism.[13] Generally, higher solution pH (under acidic) is more favorable for uptake of heavy metals onto ZrP according to earlier report.[13] The decrease of the stripping signals for Pb(II) at higher pH 4.0 may be related to the hydrolysis of heavy metal ions (Figure S3b, Supporting Information). The negative shifts of preconcentration potential (from −0.8 to −1.1 V) can obviously improve the reduction of Pb(II) and increase the peak current. When a deposition potential beyond −1.1 V is applied, a decrease in response current is observed (Figure S3c, Supporting Information). This may be due to the reduction of hydrogen leading to the formation of microgas bubbles. These bubbles decrease the effective electrode area, thereby decreasing the response of Pb(II). The peak current increases versus the accumulation time up to 150 s, indicating an enhancement in uptake of Pb(II) on electrode surface at a longer accumulation time. Because of the saturation of a modified electrode surface by Pb(II), the increase in peak current is slow when the accumulation time is longer than 150 s (Figure S3d, Supporting Information). To avoid such saturation response at high concentrations, the optimal deposition time is chosen as 120 s.

Figure 4 shows the SWASV responses of the exfoliated ZrP-modified GCE toward Pb(II) across a range of concentrations under optimal conditions. As depicted in Figure 4, the stripping peak current (i_p) is proportional to the concentration of Pb(II) in the probed range of 0.05−2.6 μM. The linearization equation is i_p (μA) = −1.02 + 31.54c (μM), with the correlation coefficients of 0.999. A high level of sensitivity of 31.54 μA μM^{-1} Pb(II) is achieved with the actual lowest detectable concentration of 0.025 μM and the statistic detection limit as low as 0.019 nM (3σ method). This meets the requirements of the World Health Organization (WHO) maximum permissible limit for lead concentration in drinking water of 10 $\mu g\ L^{-1}$.

After having detected the stripping response of Pb(II), we next attempt to detect Zn(II), Cd(II), Cu(II), and Hg(II) stripping signals using exfoliated ZrP-modified GCE under the optimal conditions (except Zn(II) deposited at −1.3 V) (Figure S4, Supporting Information). The stripping peak currents (i_p)

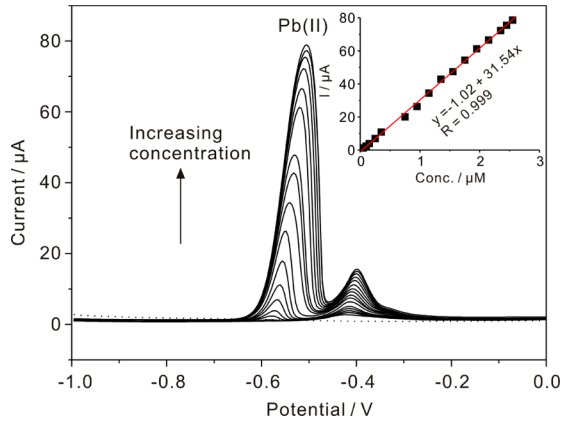

Figure 4. Typical SWASV stripping signals of Pb(II) at exfoliated ZrP-modified GCE. Stripping solution: 0.1 M NaAc−HAc, pH 4.0. SWASV conditions: deposition potential is −1.1 V; accumulation time is 120 s. The inset is the calibration plot of the SWASV peak current versus the concentration of Pb(II) ranging from 0.05 to 2.6 μM.

are proportional to the concentrations of these heavy metal ions in the probed range. Comparing these sensitivities with Pb(II), we can make a conclusion that the exfoliated ZrP-modified GCE exhibits great sensitivity toward Pb(II) than other metal ions.

The selective response of exfoliated ZrP-modified GCE is better investigated by observing the stripping signals of five heavy metal ions (Zn(II), Cd(II), Pb(II), Cu(II), and Hg(II)) in 0.1 M NaAc−HAc (pH 4.0) (Figure 5). It is apparent that

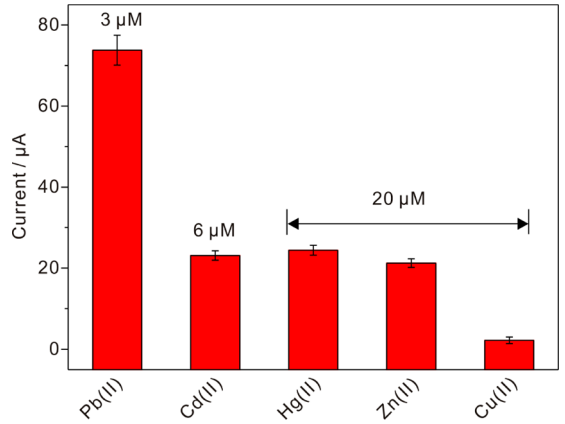

Figure 5. Voltammetric peak current of metal ions at the exfoliated ZrP-modified GCE in the presence of Pb(II), Cd(II), Hg(II), Zn(II), and Cu(II). Scanning potential range: −1.4 to +0.6 V, other conditions are identical to those in Figure 4.

the obtained stripping current toward Pb(II) is around 6 times higher than that toward Cd(II), 20−30 times higher than that toward Hg(II) and Zn(II), and 140 times higher than that toward Cu(II). This should originate from the outstanding adsorption ability of exfoliated ZrP toward Pb(II) is much stronger than those toward other heavy metal ions under the accumulation conditions.

Earlier reports indicated that ZrP exhibited favorable sorption of heavy metals particularly in terms of high selectivity toward Pb(II).[13] A series of batch equilibrium tests are carried out to confirm that the selective adsorption toward Pb(II) by exfoliated ZrP is responsible for its selective electrochemical detection. The presence of Pb, Cd, Cu, Hg, and Zn elements in

dx.doi.org/10.1021/ac3037014 | Anal. Chem. 2013, 85, 3984−3990

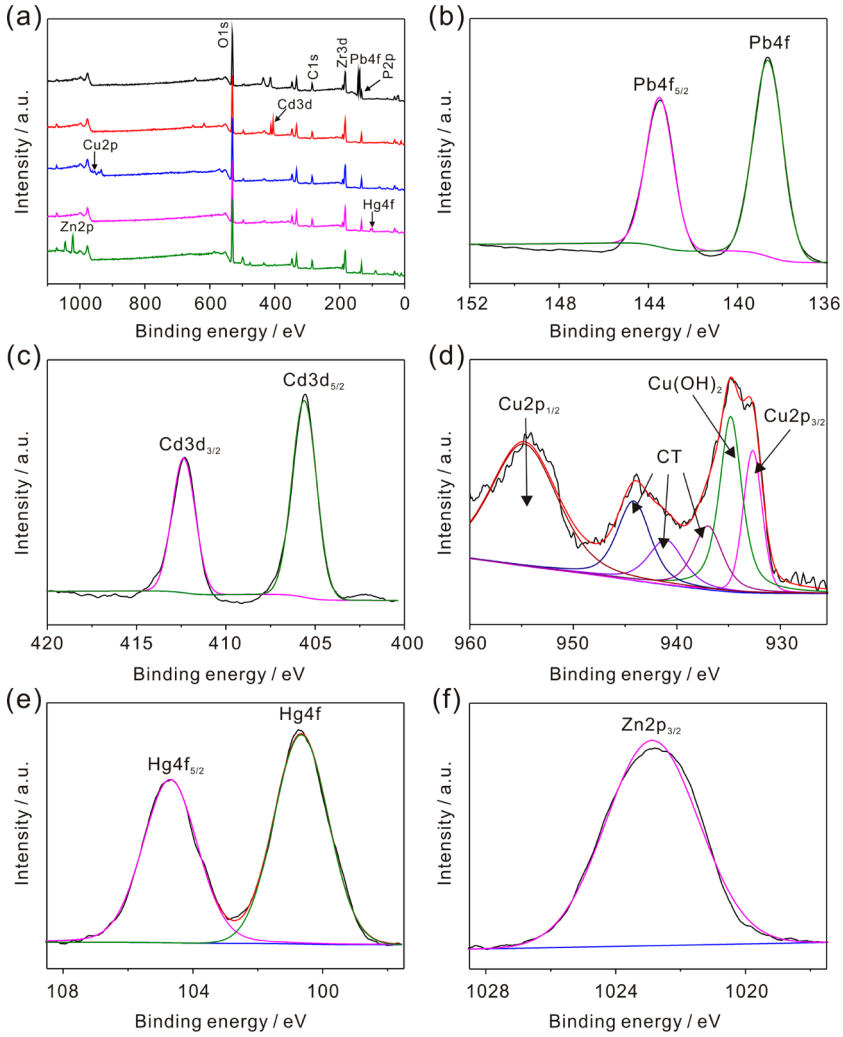

Figure 6. X-ray photoelectron spectrum: (a) full spectrum after Pb(II), Cd(II), Cu(II), Hg(II), and Zn(II) adsorption on exfoliated ZrP, (b) Pb 4f signature region, (c) Cd 3d signature region, (d) Cu 2p signature region, (e) Hg 4f signature region, and (f) Zn 2p signature region.

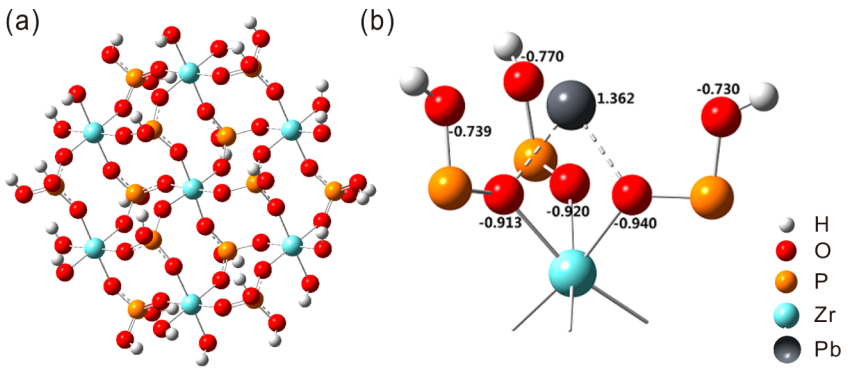

Figure 7. (a) Relaxed structure of a piece of exfoliated ZrP by freezing the outermost atoms. (b) Magnified structure with marked Mulliken charges on atoms (some coordinated oxygen atoms of P and Zr atoms are omitted for clarify.).

the exfoliated ZrP after being absorbed is further studied by X-ray photoelectron spectroscopy (XPS) (Figure 6). In full spectra (a), the XPS survey spectra reveal the presence of oxygen, carbon, zirconium and phosphorus at ~532, ~284, ~183, and ~134 eV corresponding to the O 1s, C 1s, Zr 3d, and P 2p orbitals, respectively. Besides those, there is the obvious signal for Pb, and the Pb 4f spectrum region is shown in Figure 6b. In addition, the Cd 3d (c), Cu 2p (d), Hg 4f (e), and Zn 2p (f) signature regions also display detectable signals, suggesting that all of the heavy metal ions have been adsorbed by exfoliated ZrP. The signal for Pb(II) is found to be most prominent, while the signals for other metal ions are relatively weaker but still detectable. This thus further supports that exfoliated ZrP exhibits higher adsorption capacity toward Pb(II) than toward other metal ions. Furthermore, the atomic

dx.doi.org/10.1021/ac3037014 | Anal. Chem. 2013, 85, 3984−3990

ratio of P to Zr is less than 2, which affirms that base hydrolysis takes place during the exfoliation.

It should be noted that exfoliated ZrP exhibits higher adsorption capacity toward Pb(II) than that toward other metal ions, which is consistent with the above electrochemical detections. The main reasons are that the amount of Pb(II) loaded on ZrP depends mainly upon the formation of the inner sphere complex with ZrP, while uptake of other cations is only driven by electrostatic interaction. Moreover, in general, divalent cations with low hydration energies are preferably absorbed by cation exchangers. Among all the tested cations, Pb(II) has the lowest hydration energy and is thus most preferably combined with ZrP, which partly explain the preference sequence of these metal ions.[37] Therefore, we conclude that the selective response of exfoliated ZrP originates from its highly selective adsorption.

To resolve at the atomistic level the details of the chemical interactions between heavy metal ions and exfoliated ZrP and to better and scientifically understand the microscopic adsorption mechanism, DFT calculations are carried out using the Gaussian09 suite of electronic structure programs[24] and the SIESTA Program.[25] To mimic as closely as possible the experimental condition within affordable computational cost, we take a piece of single layer α-ZrP as our explicit computational model, and the influence of the solvent environment is accounted for by the implicit solvent model. Its geometric structure of ZrP is extracted from the bulk crystal,[38] which is then relaxed with fixing the positions of the outermost Zr and P atoms to obtain the stabilized structure (Figure 7a).

Metal ions may be adsorbed on the single layer ZrP at two types of oxygen atoms: the oxygen atoms bridging the Zr and P atoms and those in the hydroxyl groups linked to the P atoms (termed as terminal oxygens). On the basis of a Mulliken charge analysis, the bridging oxygen atoms are shown to carry more negative partial charges than the terminal ones, and hence, the bridging oxygen is expected to be more favorable for adsorption of metal cations (Figure 7b). This is confirmed by the geometry optimization for the cluster model ZrP–X^{2+}, where the cation X^{2+} (X = Cu, Hg, Zn, Pb, Cd) is always bonded to two bridging oxygen atoms in a relaxed structure (see the sketch in Figure 1). Such a bonding scenario is consistent with the ion exchange mechanism suggested by previous experiments,[13,14] where adsorption of one equivalent of X^{2+} is accompanied with the release of two equivalents of proton. Before exchange occurs, each bridging oxygen atom is protonated in the acidic solution. Upon adsorption of X^{2+}, the protons on both oxygen atoms are released.

On the basis of the energetic data obtained from DFT calculations, a comparison for relative bonding energies of different metal ions is carried out as follows. By setting the absorption energy of Cu(II) as 0 kcal/mol, the relative binding energies for Hg(II), Cd(II), Zn(II), Pb(II) are 88.3, 109.1, 126.5, and 198.3 kcal/mol, respectively. The DFT calculation results verify that the exfoliated ZrP shows the strongest adsorption capability toward Pb(II) among all heavy metal ions. Therefore, the selective adsorption toward Pb(II) by exfoliated ZrP should be responsible for the selective electrochemical detection.

CONCLUSION

Exfoliated ZrP used as sensing material on the electrode surface for selective and sensitive stripping analysis of Pb(II) has been described based on the selective adsorption ability. DFT calculations were carried out to better and scientifically understand the selective adsorption resulting in selective detection. Also, the amorphous phase formation of exfoliated ZrP was illustrated via computational model for the first time. With our combined experimental and theoretical efforts, we are able to provide a new route to realize the improved selectivity in electrochemical sensing of toxic metal ions. Further experimental and computational studies about the different responses of Pb(II) in layered and exfoliated ZrP are in progress.

ASSOCIATED CONTENT

Supporting Information

Additional Information as noted in text. This material is available free of charge via the Internet at http://pubs.acs.org.

AUTHOR INFORMATION

Corresponding Author

*E-mail: xingjiuhuang@iim.ac.cn (X.-J.H.), xz58@ustc.edu.cn (X.Z.). Tel: 86-551-559-1167 (X.-J.H.). Fax: 86-551-559-2420 (X.-J.H.), 86 551 3600310 (X.Z.).

Author Contributions

‖These authors contributed equally to this work.

Notes

The authors declare no competing financial interest.

ACKNOWLEDGMENTS

This work was supported by the National Basic Research Program of China (2011CB933700), the Natural Science Foundation of China (50901073, 21073197, 21103157, and 21233007), the Fundamental Research Funds for Central Universities (2340000034), and the Youth Innovation Funds from Ministry of Education of China (2340000025).

REFERENCES

(1) Liu, M. C.; Zhao, G. H.; Tang, Y. T.; Yu, Z. M.; Lei, Y. Z.; Li, M. F.; Zhang, Y. A.; Li, D. M. *Environ. Sci. Technol.* **2010**, *44*, 4241−4246.
(2) Wang, S. P.; Forzani, E. S.; Tao, N. J. *Anal. Chem.* **2007**, *79*, 4427−4432.
(3) Chen, Y. Y.; Chang, H. T.; Shiang, Y. C.; Hung, Y. L.; Chiang, C. K.; Huang, C. C. *Anal. Chem.* **2009**, *81*, 9433−9439.
(4) Yoosaf, K.; Ipe, B. I.; Suresh, C. H.; Thomas, K. G. *J. Phys. Chem. C* **2007**, *111*, 12839−12847.
(5) Liu, J. W.; Lu, Y. *J. Am. Chem. Soc.* **2003**, *125*, 6642−6643.
(6) Schmittel, M.; Lin, H. W. *Angew. Chem., Int. Ed.* **2007**, *46*, 893−896.
(7) Lin, Z. Z.; Li, X. H.; Kraatz, H. B. *Anal. Chem.* **2011**, *83*, 6896−6901.
(8) Shen, L.; Chen, Z.; Li, Y. H.; He, S. L.; Xie, S. B.; Xu, X. D.; Liang, Z. W.; Meng, X.; Li, Q.; Zhu, Z. W.; Li, M. X.; Le, X. C.; Shao, Y. H. *Anal. Chem.* **2008**, *80*, 6323−6328.
(9) Geary, C. D.; Zudans, I.; Goponenko, A. V.; Asher, S. A.; Weber, S. G. *Anal. Chem.* **2005**, *77*, 185−192.
(10) Zhao, Z. Q.; Chen, X.; Yang, Q.; Liu, J. H.; Huang, X. J. *Chem. Commun.* **2012**, *48*, 2180−2182.
(11) Wei, Y.; Yang, R.; Zhang, Y. X.; Wang, L.; Liu, J. H.; Huang, X. J. *Chem. Commun.* **2011**, *47*, 11062−11064.
(12) Pan, D. W.; Wang, Y. E.; Chen, Z. P.; Lou, T. T.; Qin, W. *Anal. Chem.* **2009**, *81*, 5088−5094.
(13) Pan, B.; Zhang, Q.; Du, W.; Zhang, W.; Pan, B.; Zhang, Q.; Xu, Z.; Zhang, Q. *Water Res.* **2007**, *41*, 3103−3111.
(14) Pan, B. C.; Jiang, P. J.; Pan, B. J.; Zhang, W. M.; Zhang, Q. R. *Colloid Surf. A* **2008**, *322*, 108−112.

(15) Yan, Z. M.; Kirby, C. W.; Huang, Y. N. *J. Phys. Chem. C* **2008**, *112*, 8575−8586.
(16) Alberti, G.; Casciola, M.; Costantino, U.; Vivani, R. *Adv. Mater.* **1996**, *8*, 291−303.
(17) Bestaoui, N.; Spurr, N. A.; Clearfield, A. *J. Mater. Chem.* **2006**, *16*, 759−764.
(18) Kraus, K. A.; Phillips, H. O. *J. Am. Chem. Soc.* **1956**, *78*, 694−694.
(19) Liu, L.; Yang, J. F.; Li, J. P.; Dong, J. X.; Sisak, D.; Luzzatto, M.; McCusker, L. B. *Angew. Chem., Int. Ed.* **2011**, *50*, 8139−8142.
(20) Brunet, E.; Alhendawi, H. M. H.; Cerro, C.; de la Mata, M. J.; Juanes, O.; Rodriguez-Ubis, J. C. *Angew. Chem., Int. Ed.* **2006**, *45*, 6918−6920.
(21) Alberti, G.; Brunet, E.; Dionigi, C.; Juanes, O.; de la Mata, M. J.; Rodriguez-Ubis, J. C.; Vivani, R. *Angew. Chem., Int. Ed.* **1999**, *38*, 3351−3353.
(22) Sue, H. J.; Sun, L. Y.; Boo, W. J.; Clearfield, A. *New J. Chem.* **2007**, *31*, 39−43.
(23) Fang, M. M.; Kaschak, D. M.; Sutorik, A. C.; Mallouk, T. E. *J. Am. Chem. Soc.* **1997**, *119*, 12184−12191.
(24) Frisch, M. J.; Trucks, G. W.; Schlegel, H. B.; Scuseria, G. E.; Robb, M. A.; Cheeseman, J. R.; Scalmani, G.; Barone, V.; Mennucci, B.; Petersson, G. A.; Nakatsuji, H.; Caricato, M.; Li, X.; Hratchian, H. P.; Izmaylov, A. F.; Bloino, J.; Zheng, G.; Sonnenberg, J. L.; Hada, M.; Ehara, M.; Toyota, K.; Fukuda, R.; Hasegawa, J.; Ishida, M.; Nakajima, T.; Honda, Y.; Kitao, O.; Nakai, H.; Vreven, T.; Montgomery, J. A., Jr.; Peralta, P. E.; Ogliaro, F.; Bearpark, M.; Heyd, J. J.; Brothers, E.; Kudin, K. N.; Staroverov, V. N.; Kobayashi, R.; Normand, J.; Raghavachari, K.; Rendell, A.; Burant, J. C.; Iyengar, S. S.; Tomasi, J.; Cossi, M.; Rega, N.; Millam, N. J.; Klene, M.; Knox, J. E.; Cross, J. B.; Bakken, V.; Adamo, C.; Jaramillo, J.; Gomperts, R.; Stratmann, R. E.; Yazyev, O.; Austin, A. J.; Cammi, R.; Pomelli, C.; Ochterski, J. W.; Martin, R. L.; Morokuma, K.; Zakrzewski, V. G.; Voth, G. A.; Salvador, P.; Dannenberg, J. J.; Dapprich, S.; Daniels, A. D.; Farkas, Ö.; Ortiz, J. V.; Cioslowski, J.; Fox, D. J. *Gaussian 09*, revision A.02 ; Gaussian, Inc.: Wallingford, CT, 2009.
(25) Soler, J. M.; Artacho, E.; Gale, J. D.; Garcia, A.; Junquera, J.; Ordejon, P.; Sanchez-Portal, D. *J. Phys-Condens. Matter* **2002**, *14*, 2745−2779.
(26) Becke, A. D. *J. Chem. Phys.* **1993**, *98*, 1372−1377.
(27) Lee, C. T.; Yang, W. T.; Parr, R. G. *Phys. Rev. B* **1988**, *37*, 785−789.
(28) Tomasi, J.; Mennucci, B.; Cammi, R. *Chem. Rev.* **2005**, *105*, 2999−3093.
(29) Perdew, J. P.; Burke, K.; Ernzerhof, M. *Phys. Rev. Lett.* **1996**, *77*, 3865−3868.
(30) Kaschak, D. M.; Johnson, S. A.; Hooks, D. E.; Kim, H. N.; Ward, M. D.; Mallouk, T. E. *J. Am. Chem. Soc.* **1998**, *120*, 10887−10894.
(31) Alberti, G.; Marmottini, F. *J. Colloid Interface Sci.* **1993**, *157*, 513−515.
(32) Meng, Y. Z.; Hu, H.; Martin, J. C.; Xiao, M.; Southworth, C. S.; Sun, L. Y. *J. Phys. Chem. C* **2011**, *115*, 5509−5514.
(33) Kim, H. N.; Keller, S. W.; Mallouk, T. E.; Schmitt, J.; Decher, G. *Chem. Mater.* **1997**, *9*, 1414−1421.
(34) Sue, H. J.; Sun, L. Y.; Boo, W. J.; Sun, D. H.; Clearfield, A. *Chem. Mater.* **2007**, *19*, 1749−1754.
(35) Boo, W. J.; Sun, L. Y.; Liu, J.; Moghbelli, E.; Clearfield, A.; Sue, H. J.; Pham, H.; Verghese, N. *J. Polym. Sci .Pol. Phys.* **2007**, *45*, 1459−1469.
(36) Hutton, L. A.; Newton, M. E.; Unwin, P. R.; Macpherson, J. V. *Anal. Chem.* **2011**, *83*, 735−745.
(37) Zhang, Q. R.; Du, W.; Pan, B. C.; Pan, B. J.; Zhang, W. M.; Zhang, Q. J.; Xu, Z. W.; Zhang, Q. X. *J. Hazard. Mater.* **2008**, *152*, 469−475.
(38) Troup, J. M.; Clearfield, A. *Inorg. Chem.* **1977**, *16*, 3311−3314.